RESEARCH ARTICLE SUMMARY

EVOLUTION

Experimental evolution of evolvability

Michael Barnett*, Lena Meister, Paul B. Rainey*

INTRODUCTION: The capacity to generate adaptive variation is critical for long-term evolutionary success. However, the extent to which natural selection directly favors enhanced evolvability remains debated. Although studies with microbes show that mutants with elevated genome-wide mutation rates can be selected, a deeper question persists: Can natural selection structure genetic and developmental systems to bias mutations toward adaptive outcomes? This hypothesis challenges the traditional view of evolution as a "blind" process fueled by random variation, which amplifies traits beneficial in the present without regard for future contingencies.

RATIONALE: Mutation being biased toward adaptive outcomes challenges conventional perspectives but aligns with the logic of natural selection acting on lineages. Across changing environments, lineages capable of rapid adaptation are more likely to survive and replace those less able. If competing lineages, because of their varying genetic architecture, tend to generate phenotypic variation in different ways, then those with tendencies that are more conducive to an adaptive response in a given environment will be favored. Provided the same environmental challenges recur over time, an iterative process of selection can take place, potentially refining the capacity to adapt. To test this idea, we designed an experiment where lineages of bacteria competed to repeatedly achieve, through mutation, phenotypes optimal for growth under two alternating conditions. Lineages that failed to evolve the target phenotype within a set time went extinct and were replaced by successful lineages. This birth-death dynamic created conditions for selection to refine the ability of lineages to evolve between phenotypic states.

RESULTS: During the course of a 3-year selection experiment, involving identification and ordering of more than 500 mutations, a lineage emerged that was capable of rapid mutational transitions between alternate phenotypic states through localized hypermutation. The mutable locus arose through a multistep evolutionary process: Initial mutations targeted a wide range of genes but eventually focused on a single regulator. A series of mutations that alternately activated and inactivated function of the regulatory gene then followed. A subset of these inactivating mutations were compensated for by mutations that increased transcription and, concomitantly, frameshift mutation rate. The overall effect was to promote, through slipped-strand mispairing, the duplication, and then further amplification, of a heptanucleotide sequence. This process led the locus-specific mutation rate to increase ~10,000-fold. In turn, the resulting frameshift mutations enabled reversible phenotypic changes through expansion and contraction of the heptanucleotide sequence, mirroring the contingency loci of pathogenic bacteria. Lineages with the hypermutable locus exhibited enhanced evolvability to altered rates of environmental change and were more likely to acquire additional adaptive mutations, highlighting an unanticipated evolutionary advantage of localized hypermutability.

CONCLUSION: Our study demonstrates how selection can incorporate evolutionary history into the genetic architecture of a single cell, giving rise to a hypermutable locus that appears to anticipate environmental change, thereby accelerating adaptive evolution. This was possible only as an outcome of selection working at two levels. Whereas individual-level selection repeatedly drove cell populations between the same two phenotypic states, the genetic underpinnings of these phenotypes were free to diverge, fueling an exploration of evolutionary potential, the consequences of which only emerged on the timescale of lineages. Ultimately, this exploration generated the variation necessary for construction and cumulative refinement of a lineage-level adaptive trait. More generally, our experiment clarifies the conditions by which evolvability can itself evolve adaptively and highlights the importance of this process for microbial pathogens. ■

The list of author affiliations is available in the full article online.
*Corresponding author. Email: barnett@evolbio.mpg.de (M.B.); rainey@evolbio.mpg.de (P.B.R.)
Cite this article as M. Barnett *et al.*, *Science* **387**, eadr2756 (2025). DOI: 10.1126/science.adr2756

READ THE FULL ARTICLE AT
https://doi.org/10.1126/science.adr2756

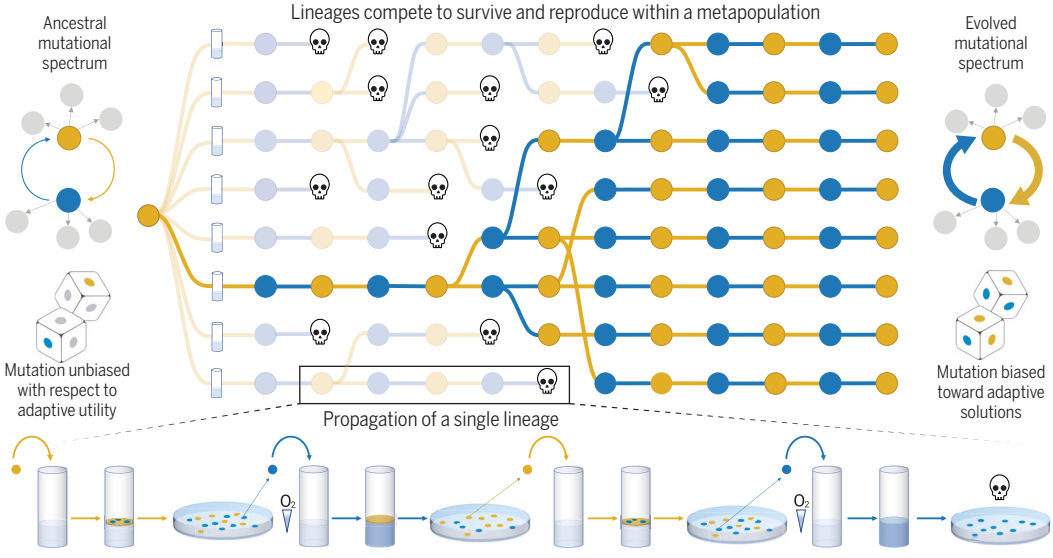

Experimental evolution of evolvability through lineage selection. Mutation and selection are typically viewed as independent processes, but our experiment revealed how they interact, leading mutation to become biased toward adaptive outcomes. Central to this was lineage-level selection: Bacterial lineages (connected nodes) were required to repeatedly evolve between two phenotypic states (indicated by yellow and blue). Mutational transitions were initially unreliable, leading to lineage death (indicated by a skull) and replacement by more successful competitors. Final surviving lineages evolved mutation-prone sequences in a key gene underpinning the phenotypes, enabling rapid transitions between states.

RESEARCH ARTICLE

EVOLUTION

Experimental evolution of evolvability

Michael Barnett[1]*, Lena Meister[1], Paul B. Rainey[1,2]*

Evolvability—the capacity to generate adaptive variation—is a trait that can itself evolve through natural selection. However, the idea that mutation can become biased toward adaptive outcomes remains controversial. In this work, we report the evolution of enhanced evolvability through localized hypermutation in experimental populations of bacteria. The evolved mechanism is analogous to the mutation-prone sequences of contingency loci observed in pathogenic bacteria. Central to this outcome was a lineage-level selection process, where success depended on the capacity to evolve between two phenotypic states. Subsequent evolution showed that the hypermutable locus is itself evolvable with respect to alterations in the frequency of environmental change. Lineages with localized hypermutability were more likely to acquire additional adaptive mutations, revealing an unanticipated benefit.

Evolvability—the capacity to generate adaptive variation—can be shaped by natural selection. Direct evidence comes from experimental studies of evolution in microbes where mutants with elevated genome-wide mutation rates are favored by selection because of their increased likelihood of finding beneficial variants (*1*–*5*). Evolvability in this sense is readily understood. Less clear, and often controversial, is whether (and how) selection might structure genetic and developmental systems so that mutation becomes biased toward adaptive outcomes (*6*–*8*).

One reason for skepticism stems from the fact that natural selection amplifies traits beneficial in the present environment and is "blind" to future contingencies. Thus, the suggestion that selection might structure organisms to evolve in directions that facilitate future adaptation is problematic. And yet, environmental change can exhibit regularities over evolutionary timescales that, in theory, might lead to biased patterns of variability (*9*, *10*). Indeed, in silico evolving populations experiencing selection toward varying and recurring goals show improved capacity to reach these goals over time (*11*–*15*). This is achieved by evolving genotype-phenotype mappings in which states adaptive in the past become more readily generated by mutation. Therefore, should future selective environments resemble past ones, derived types become biased toward generating adaptive change.

A compelling case for evolvability in this sense is found in the so-called contingency loci of pathogenic bacteria (*16*). These loci are characterized by the presence of mutation-prone sequences, such as short-sequence repeats, in genes that encode products that determine interactions with the external environment. Such hypermutable loci cause descendant cells to achieve a diverse, yet biased, set of phenotypic states, central to persistence in the face of challenges presented by host immune responses (*17*).

Although a history of repeated encounters with a selective environment dispels any mystery of foresight, certain traits that facilitate adaptive evolution, such as contingency loci, remain difficult to explain without invoking selection operating above the individual level. This is problematic because conditions necessary for selection at higher levels are assumed to be rare, which limits possibilities for the cumulative refinement of higher-level adaptive traits (*6*, *8*, *18*). Nevertheless, the fundamental logic of natural selection is indifferent to level of organization or timescale, and provided that variation, reproduction, and heredity exist, selection can shape traits that are adaptive at levels beyond the individual (*19*).

Consider, for example, competition between lineages that vary in their capacity to generate adaptive variation. Across changing environments, those less evolvable are likely to face extinction, whereas more evolvable lineages not only survive but can also expand to colonize the space occupied by extinct lineages. This constitutes a form of lineage reproduction. Selection here works over two timescales: on individuals, favoring those with adaptive phenotypes, and on lineages, favoring those whose properties enabled the generation of adaptive phenotypes. Differential reproductive success of lineages that vary in evolvability generates selection that can refine traits that promote lineage survival and reproduction (*20*–*25*).

Results

We asked whether a selective regime imposed on lineages that rewarded capacity to generate adaptive phenotypic variation would result in the evolution of lineages with enhanced evolvability. To this end, we exploited cyclical evolutionary dynamics of the bacterium *Pseudomonas fluorescens* to provoke repeated phenotypic transitions between two niche specialist mutants (*26*): the mat-forming, cellulose-overproducing CEL^+ type and the mat-colonizing, non–cellulose-producing CEL^- type. We then challenged lineages to repeatedly evolve between the two phenotypic states. Lineages that failed to produce cells of the necessary state were replaced by those that were successful (Fig. 1).

Adaptive evolution of lineages

The regime shown in Fig. 1 ensures that selection works on both cells and lineages. Although each metapopulation starts from a single genotype, unique mutational paths taken to transition between phenotypic states create variation between lineages. Such mutations change the phenotype in an equivalent way but likely differ in their effects on the chance and impact of future mutations. Lineages thereby begin to vary in evolutionary potential. An inability to reach the next adaptive target results in lineage extinction and the opportunity for successful lineages to "reproduce" through replacement. Lineages that vary in evolvability thereby compete to survive and reproduce within a metapopulation, with opportunity for evolvability-enhancing traits to be amplified and cumulatively refined by lineage-level selection.

Knowledge of the fate of lineages within metapopulations allows precise depiction of evolutionary dynamics (Fig. 2). "Selective sweeps" are evident in three of the four metapopulations (A to C) in which descendants of single lineages proliferate and form unbroken series of successful transitions, indicating a decreased extinction rate. Metapopulation D suffered a mass extinction at transition 48. If lineages had not been treated as units of selection, that is, if in the face of extinction, reproduction of viable lineages had been disallowed, then all metapopulations would have faced early extinction (fig. S1).

Whole-genome sequences of derived lineages from metapopulations were obtained at the end point of each series and en route. In metapopulations A and C (Fig. 2), derived lineages were found to carry loss-of-function mutations in genes involved in mutational repair (*mutS* and *uvrD*, respectively), with the point of origin marked in Fig. 2. An assay of global mutation rates in metapopulations A and C showed these to be elevated 300- and 350-fold, respectively, indicating that the adaptive response of lineages was underpinned by global hypermutability. By contrast, no mutations affecting genes involved in DNA replication or repair were detected in metapopulation B, and global mutation rates remained unchanged (fig. S2).

[1]Department of Microbial Population Biology, Max Planck Institute for Evolutionary Biology, Plön, Germany. [2]Laboratory of Biophysics and Evolution, CBI, ESPCI Paris, Université PSL, CNRS, Paris, France.
*Corresponding author. Email: barnett@evolbio.mpg.de (M.B.); rainey@evolbio.mpg.de (P.B.R.)

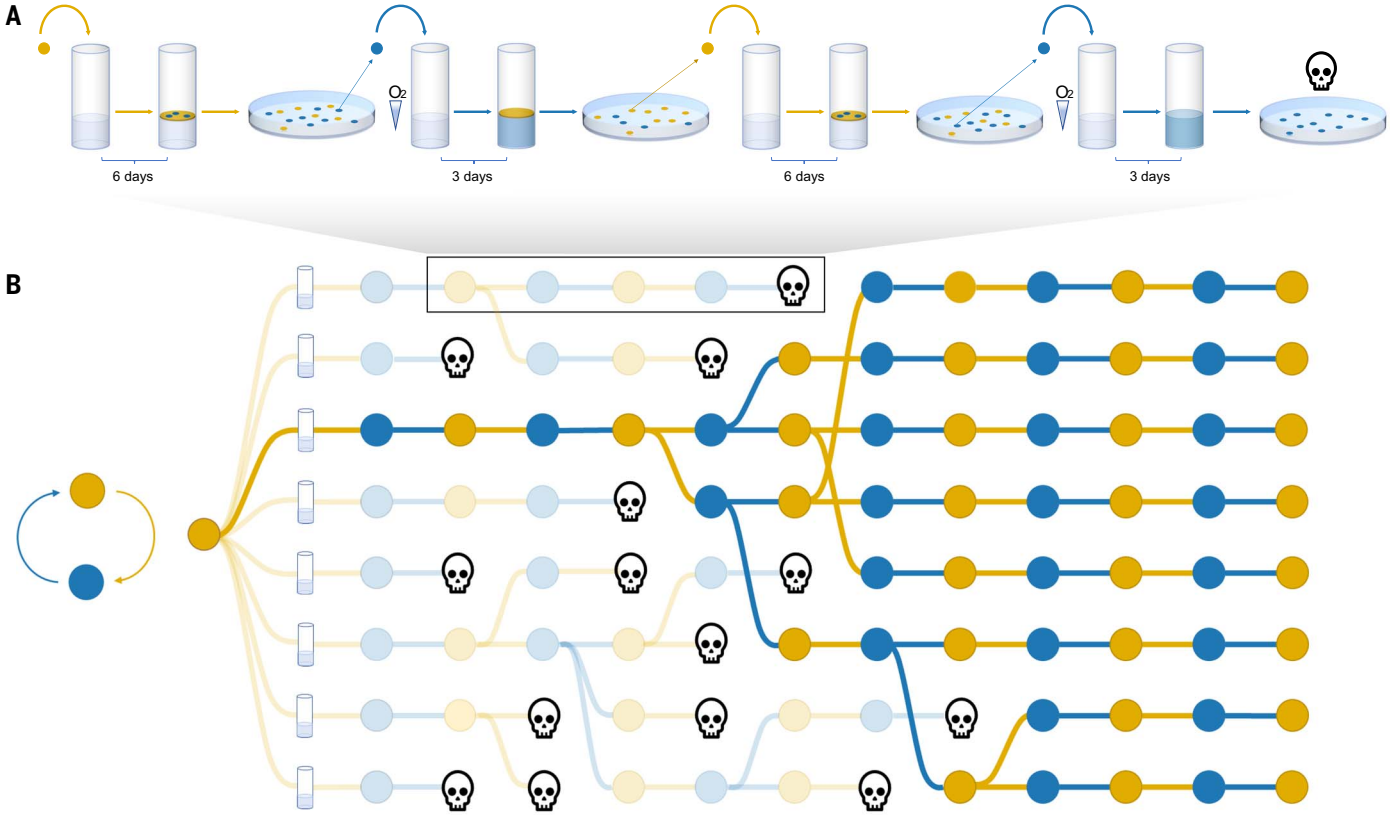

Fig. 1. Lineage selection. (**A**) Experimental protocol that begins by founding a microcosm with a single CEL$^+$ genotype (yellow circle). After 6 days in static culture, descendant cells are diluted and plated on agar, with colony phenotype allowing detection of CEL$^-$ mutants (blue circles). A single CEL$^-$ mutant is then used to found growth in a fresh microcosm, with a sample again examined by agar plate culture for the presence of CEL$^+$ types. A single CEL$^+$ type then founds the next bout of selection, and the cycle repeats. Selective bottlenecks ensure that the next phenotypic state must be generated afresh through mutation; propagation of single colonies enables precise tracking of lineages. In this example, representing the highlighted section of (B), the lineage goes extinct on the final transfer because it failed to generate the next (CEL$^+$) target phenotype. Key to the selection regime are frequency-dependent interactions between the two phenotypes: CEL$^+$ forms a mat at the surface and provides conditions that favor CEL$^-$ mutants; CEL$^-$ types deplete oxygen, thus establishing conditions that favor the evolution of surface-colonizing CEL$^+$ types. (**B**) Graphical representation of the lineage-selection regime in which multiple lineages (connected circles) compete to survive and reproduce within a metapopulation. Survival requires repeated transitions between the CEL$^+$ (yellow) and CEL$^-$ (blue) phenotypes by mutation. Lineages that fail to achieve the target phenotype are marked extinct (indicated by a skull), with extinction providing opportunity for replacement by a randomly selected extant lineage. Depicted is an example of a lineage that has evolved increased evolvability, leading to a decreased likelihood of extinction and fixation of the lineage in the metapopulation.

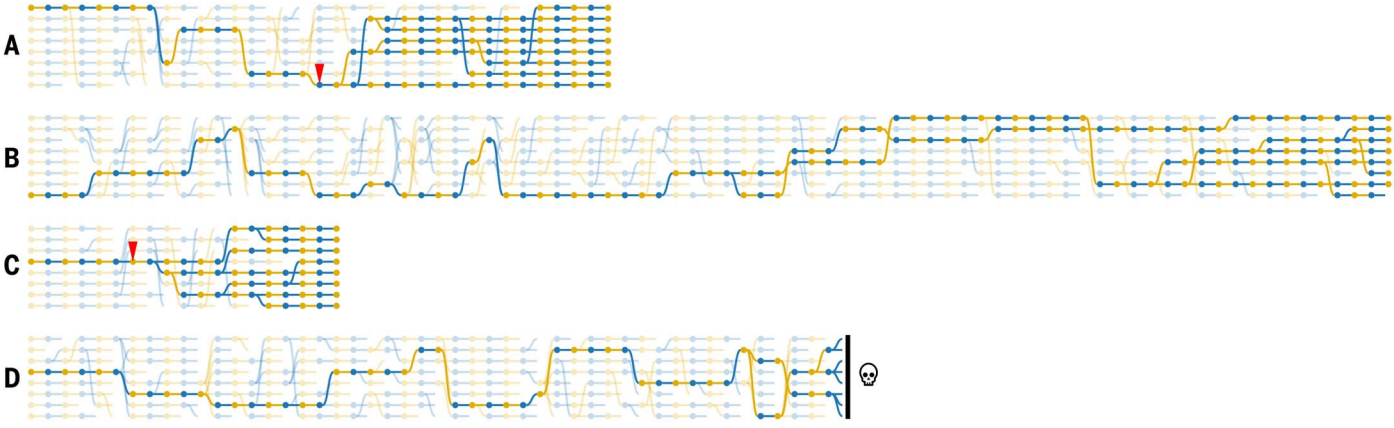

Fig. 2. Evolutionary dynamics of metapopulations. Four CEL$^+$ genotypes were used to separately found four metapopulations (**A** to **D**), each of which are composed of eight lineages. Yellow nodes indicate the CEL$^+$ target phenotype and blue nodes indicate CEL$^-$. Lineage death occurred through failure to generate the target phenotype and provided extant lineages opportunity for birth. Solid lines depict the genealogy of final surviving lineages, with extinctions indicated by broken faded lines. Red arrows in metapopulations A and C indicate the point of origin of mutator genotypes that founded lineages that rapidly fixed.

Local hypermutability underpins lineage adaptation

Metapopulation B ultimately cycled through 80 transitions (720 days within microcosms), with the experiment being terminated after stable persistence of a single lineage. To understand the genetic basis of success, whole-genome resequencing was used to identify and order mutations underpinning each transition between the CEL$^+$ and CEL$^-$ states. This revealed 548 mutational events that targeted 84 genes, 34 of which were hit multiple times. Common targets included various regulators of cyclic-di–guanosine monophosphate (cyclic-di-GMP) (394 of 548)—the intracellular signaling molecule that activates the synthesis of cellulose-generating CEL$^+$—and mutations to the cellulose biosynthesis machinery itself (67 of 548). The diversity of mutational paths generated variation in evolutionary potential between lineages, with many lineages following routes that became genetic dead ends [detailed in figs. S3 and S4; an interactive dataset for metapopulation B is available online (*27*)].

Despite the availability of possible mutational paths, a single regulatory gene, *pflu0185*, became the main mutational target, eventually accounting for 59% (306 of 520) of all phenotypic transitions. Moreover, most of these (186 of 306) were caused by duplication or loss of a heptanucleotide (HN) sequence "GGTGCCC" located near the 5′ end of the gene (nucleotides 19 to 25). Mapping the occurrence of transitions caused by changes in copy number of the HN sequence on dynamics of lineages within metapopulation B (Fig. 3C) showed that these mutations were associated with a decrease in the number of extinctions from 26% per transition to 10% (Fig. 3A), indicating that this locus underpinned lineage adaptation.

Mechanistically, rapid changes in the number of copies of short sequence repeats can be attributed to slipped-strand mispairing—a genomic instability that increases the likelihood of deleting or duplicating repeated units (*28*). This occurs when DNA strands spontaneously dissociate but reanneal with an adjacent repeat unit. Relevant here is the sequence of nucleotides immediately downstream of the duplicated HN sequence (GGTGCCC): In ancestral *pflu0185*, there exists a further copy of GGTG and thus the focal sequence is GGTG-CCCGGTG (Fig. 3D). Mispairing between the two copies of GGTG causes the interstitial CCC to be copied, resulting in the initial HN duplication. Addition of the HN sequence disrupts the *pflu0185* reading frame near its N terminus, preventing translation of functional protein.

Pflu0185 is a regulatory protein composed of two enzymatic domains: a diguanylate cyclase (DGC), responsible for the synthesis of cyclic-di-GMP, and a phosphodiesterase (PDE), responsible for its breakdown (*29*). In *P. aeruginosa*, functional analysis showed the protein to have PDE function but no DGC activity (*30*). This is consistent with the genetic analysis reported here. As a consequence of the initial HN duplication, PDE function is lost and cyclic-di-GMP levels increase within the cell. Elevated levels of cyclic-di-GMP in turn activate the cellulose biosynthesis machinery, and cells enter the CEL$^+$ state.

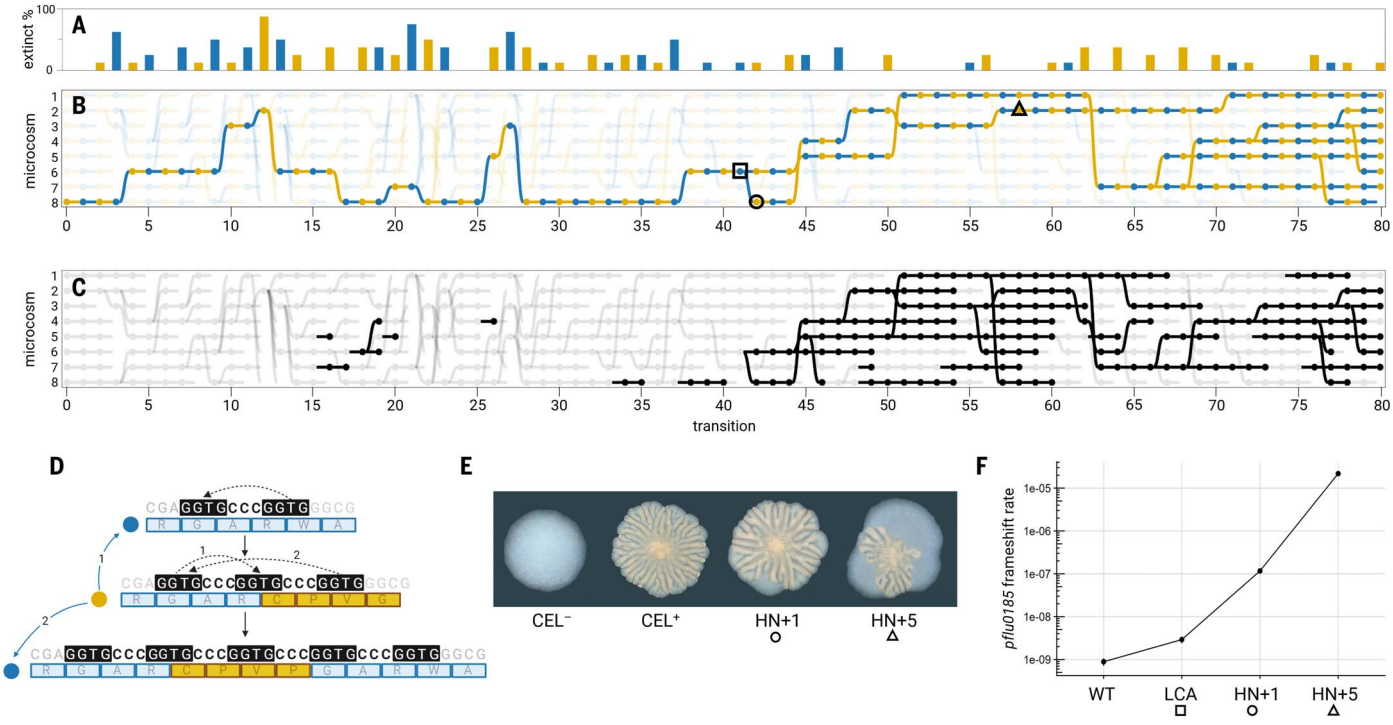

Fig. 3. Localized hypermutability accounts for adaptive advantage of derived lineages in metapopulation B. (**A**) Extinction events at CEL$^+$ (yellow) and CEL$^-$ (blue) transitions. (**B**) Lineage dynamics with focal points indicated by symbols around nodes. The *x*-axis labels are transitions (T), and the *y* axes denote microcosm (M). The node identified by the open black square is thus T41 M6. (**C**) Phenotypic transitions effected by changes in the number of copies of a HN sequence in *pflu0185*. (**D**) Proposed mechanism of slipped-strand mispairing. The top graphic shows the DNA sequence of *pflu0185* surrounding, and including, the focal HN sequence (GGTGCCC) plus relevant downstream nucleotides (GGTG). The dotted arrow indicates mispairing between GGTG repeats, which leads to an additional copy of the HN sequence (middle, vertical arrow). With two copies of the HN sequence, the reading frame is destroyed. The reading frame can be corrected by either mispairing in the forward direction (dotted arrow 1), which restores the original state (blue arrow 1), or by mispairing in the reverse direction (dotted arrow 2), resulting in four copies of the HN sequence (bottom, vertical arrow). (**E**) Image of CEL$^-$ and CEL$^+$ colonies after prolonged (72 hours) growth on agar plates, with derived lineages having either a single additional copy of the HN sequence or five additional copies; the latter show overt sectoring indicative of an elevated mutation rate. (**F**) Relationship between genotype and rate of frameshift mutations in *pflu0185*. Symbols denote genotypes from (B). Error bars (largely contained within the points) are 95% CI. WT, wild type; LCA, last common ancestor.

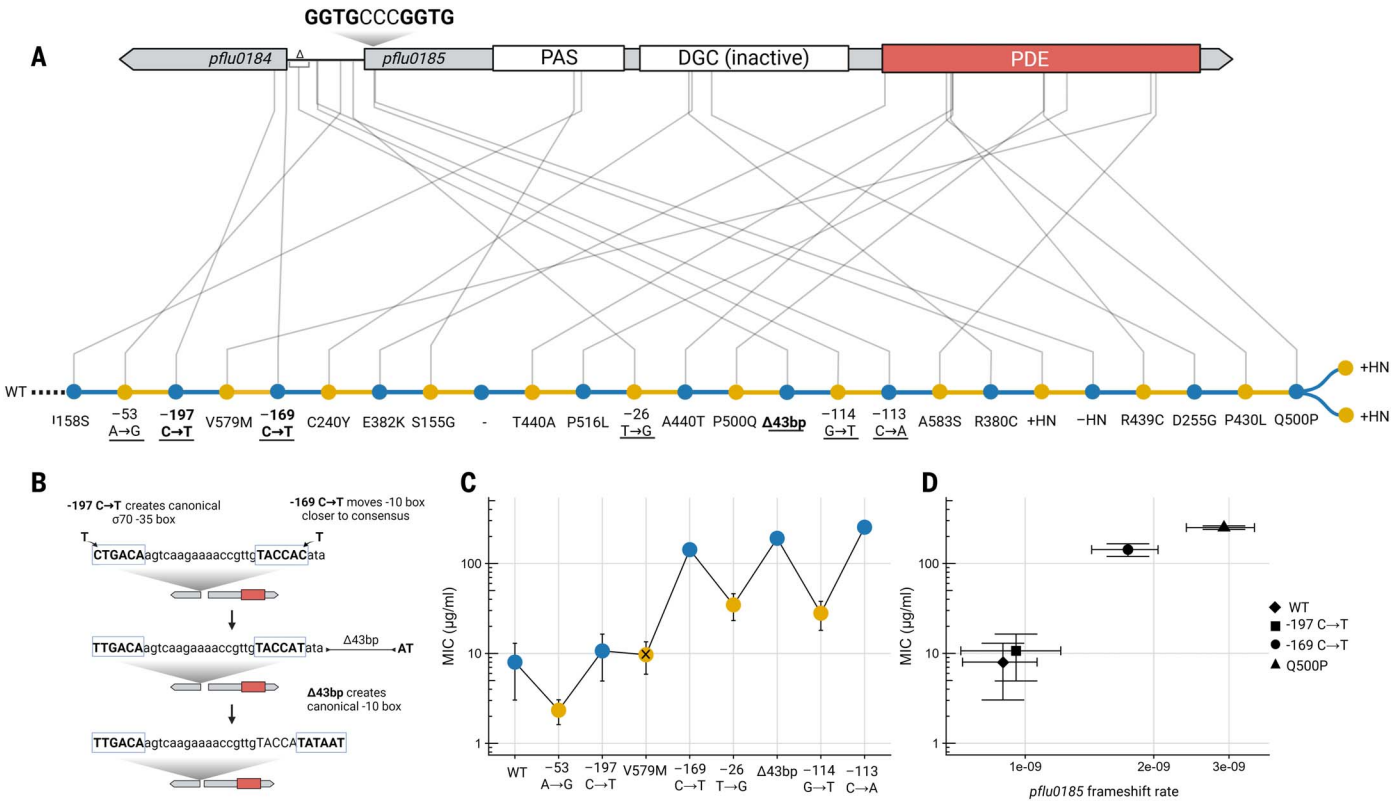

Fig. 4. Mutational history of potentiating mutations in *pflu0185*. (**A**) Genetic structure of *pflu1085* and sequence of successive mutations modulating changes in phenotypic state. Shown at the top is the *pflu0185* open reading frame indicating the locations of the HN sequence, PAS signaling domain, inactive DGC domain, and, in red, the PDE domain. Also shown is the upstream gene and intergenic space where multiple mutations arose that affected transcription. [Figure created with BioRender.com] (**B**) Mutational changes in upstream regions (in bold type) placed in the context of surrounding DNA sequence that contribute to formation of a typical *Pseudomonas* promoter (*63*, *64*). [Figure created with BioRender.com] (**C**) Effects of mutations on the transcription of *pflu0185* and CEL^+ or CEL^- status determined through assay of MIC in the presence of kanamycin [putative promoter mutations are underlined in (A)]. Mutation V579M (Val^{579}→Met; marked with a cross) is included to demonstrate its role in reducing catalytic activity of the PDE, necessitating further increases in *pflu0185* transcription. (**D**) Relationship between transcription (as determined by MIC assay) and rate of frameshift mutations in *pflu0185*. Note that the MIC of Q500P (Gln^{500}→Pro) is equivalent to the last occurring upstream mutation (−113 C→A). Error bars are 95% CIs. Single-letter abbreviations for the amino acid residues represented in mutation notations are as follows: A, Ala; C, Cys; D, Asp; E, Glu; F, Phe; G, Gly; H, His; I, Ile; K, Lys; L, Leu; M, Met; N, Asn; P, Pro; Q, Gln; R, Arg; S, Ser; T, Thr; V, Val; W, Trp; and Y, Tyr.

Beyond the adaptive CEL^+ phenotype, cells that inherited the initial HN duplication in *pflu0185* also inherited an enhanced ability to generate the CEL^- phenotype, being ~5-fold more likely to survive the next transition than cells that inherited any other mutation {95% confidence interval (CI) [1.8, 12.9], $P = 0.0006$, Fisher's exact test, two-tailed}. This increased survival can be explained by the relationship between the number of tandem repeats and the rate of mispairing, where a rise in the number of repeats is expected to elevate the local mutation rate (*17*). The effect is that cells with the HN duplication are primed to reactivate *pflu0185* function through indels that restore the reading frame. Indeed, 96% of lineages that inherited the initial duplication corrected the reading frame through subsequent expansion or contraction of the HN repeat. In 86 instances, this involved restoration of the reading frame by contraction and, only in three instances, through expansion by addition of two HN copies. However, lineages that expanded the tract were then more likely to see further expansion in copy number of the HN sequence at the next transition (5:3 contraction:expansion, $P = 0.0049$, Fisher's exact test, two-tailed). As the number of repeats increased, the rate at which transitions occurred visibly increased (Fig. 3E).

Although global measures of mutation rate (fig. S2) showed no increase, by fusing *pflu0185* to an out-of-frame kanamycin resistance (*kanR*) gene, the rate of frameshifting, specifically within *pflu0185*, was quantified (Fig. 3F). A statistically significant threefold increase in the rate of frameshifting was evident in the genotype that marked the coalescent point of the final lineages (T41 M6; open black square in Fig. 3B), despite the fact that this genotype carried no additional copy of the HN sequence. With two (+1) copies (T42 M8; open black circle in Fig. 3B), the rate of frameshifting increased a further 150-fold, and with six (+5) copies (T58 M2; open black triangle in Fig. 3B) (the maximum observed in the selection experiment), the rate of frameshifting was more than four orders of magnitude greater than the ancestral genotype (Fig. 3F).

Elevated transcription-potentiated repeat-associated hypermutation

Having established localized hypermutability as underpinning lineage adaptation in metapopulation B, we next sought further understanding of its evolutionary origins. In particular, questions remained as to why initial duplication of the HN sequence had become increasingly probable, despite any loss of function within *pflu0185* being capable of achieving the same effect. Indeed, alternative loss-of-function mutations in *pflu0185* were still occasionally observed late in evolution and, where irreparable, led to lineage extinction (fig. S5).

Our focus therefore turned to the series of mutations targeting *pflu0185* that occurred

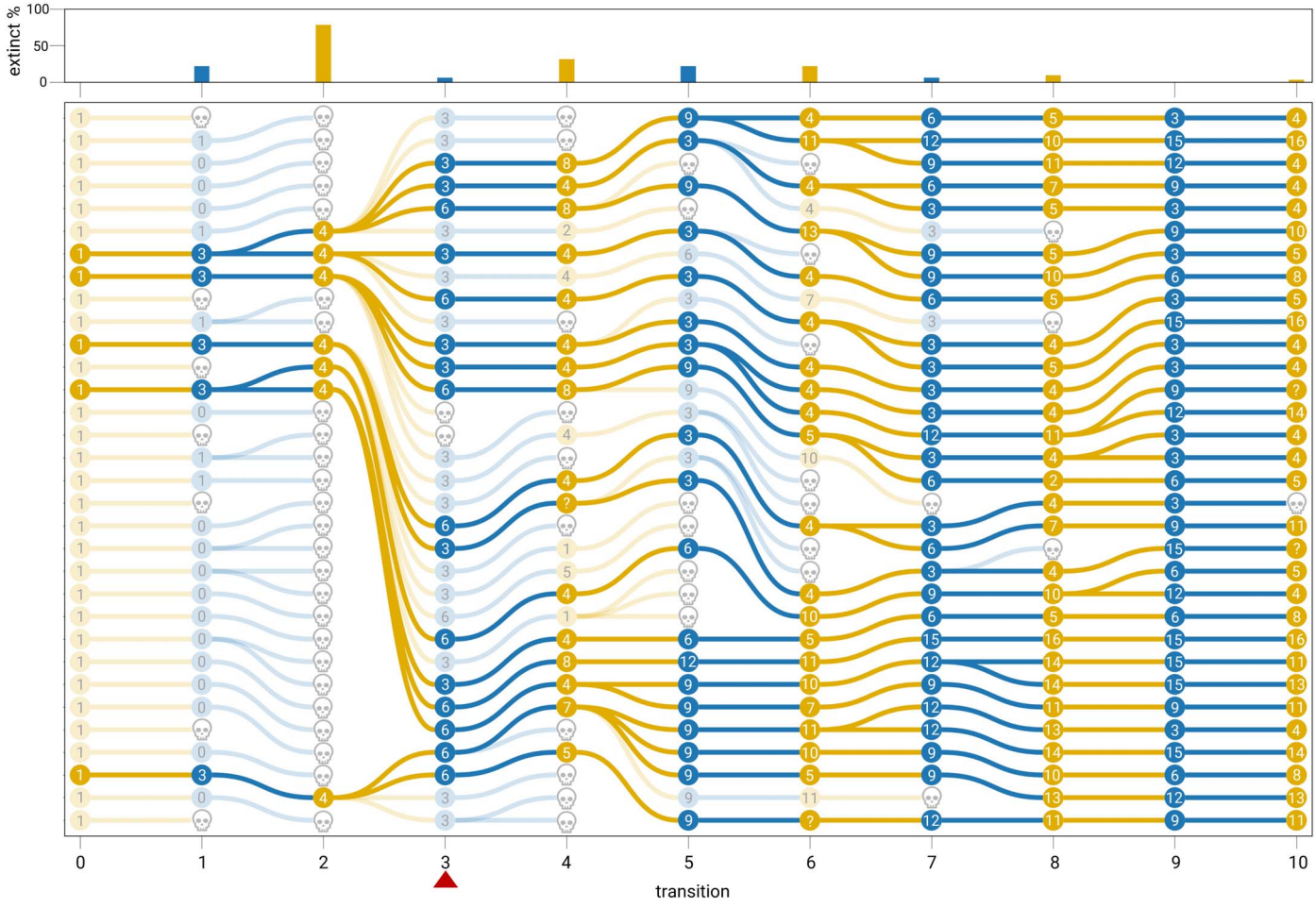

Fig. 5. Stringent selection drives expansion in HN copy number. A total of 32 lineages were founded by genotype T42 M8 (open black circle in Fig. 3B), which contains a single additional copy of the HN sequence. Lineages were subject to the selection regime shown in Fig. 1, but population size was reduced 30-fold and lineages were required to achieve the target phenotype within 24 hours or face extinction. The number of additional HN units over the ancestral *pflu0185* sequence is indicated within nodes. Phenotypic states are CEL^+ (yellow) and CEL^- (blue). The red triangle indicates a point after which the stringency of selection was further increased by requiring successful lineages to have at least five colonies of the target phenotype present. The top panel shows extinctions at each transition.

before the expansion of lineages at T41 M6. By this point, *pflu0185* had acquired 24 mutations (including three direct reversals), either within or upstream of the gene, with each mutation being responsible for the transition between the CEL^+ and CEL^- states (Fig. 4A). No single event stood out in terms of relevance to hypermutability caused by changes in copy number of the HN sequence. However, notable were multiple mutations targeting the upstream region, with some leading to formation of promoter motifs, indicating a role in transcription (Fig. 4B). Considering the mutagenic nature of transcription (*31*), we examined the dual effects of upstream mutations on the levels of transcription and rate of frameshifting in *pflu0185*.

To assess effects of mutations on *pflu0185* transcription, we took advantage of the *pflu0185-kanR* gene fusion, using level of kanamycin resistance [expressed as minimum inhibitory concentration (MIC)] as a proxy. This revealed a ratcheting effect of mutations, with those causing either a reduction in transcription of *pflu0185* or a reduction in catalytic activity of the PDE (leading to the CEL^+ state) being compensated for by mutations in the upstream region that elevated transcription (leading to the CEL^- state) (Fig. 4C). By the end of this series of mutations, transcription of *pflu0185* was elevated 30-fold above that of ancestral *P. fluorescens*.

In terms of the possibility that these mutations had potentiated the proclivity of the HN sequence to expand in copy number, the relationship between MIC and the rate of frameshift mutations in *pflu0185* was determined. This revealed a positive correlation (Fig. 4D). Notably, a promoter mutation activating *pflu0185* also preceded the first instances of mutation via the HN sequence, which occurred independently in a sublineage that later went extinct (T16 M5 and T16 M7 in Fig. 3C). Previous assays of global mutation rates were insensitive to frameshift mutations, so we therefore measured the rate of frameshifting using the out-of-frame kanamycin resistance gene reporter but placed in a different genomic context. This showed no significant elevation in frameshifting (fig. S5), confirming the local nature of elevated frameshifting in *pflu0185*.

Stringent selection drives expansion of repeats

Despite the potential for self-accelerating increases in mutation rate by successive duplication of repeats, all lineages that expanded the HN sequence periodically reverted to a single copy. This meant that lineages often relied on the relatively low rate of initial HN duplication for survival. Consequently, extinction events persisted, primarily because of CEL^- transitions mediated by destruction of the cellulose biosynthesis machinery (fig. S6).

We reasoned that this tendency was in part a consequence of high mutation supply within microcosms (a product of population size and propagation time), which meant extreme mutation rates (Fig. 3F) were not necessary to reliably generate cells with the target phenotype. Indeed, contingency loci found in nature often consist of many tandem repeats (*17*), suggesting

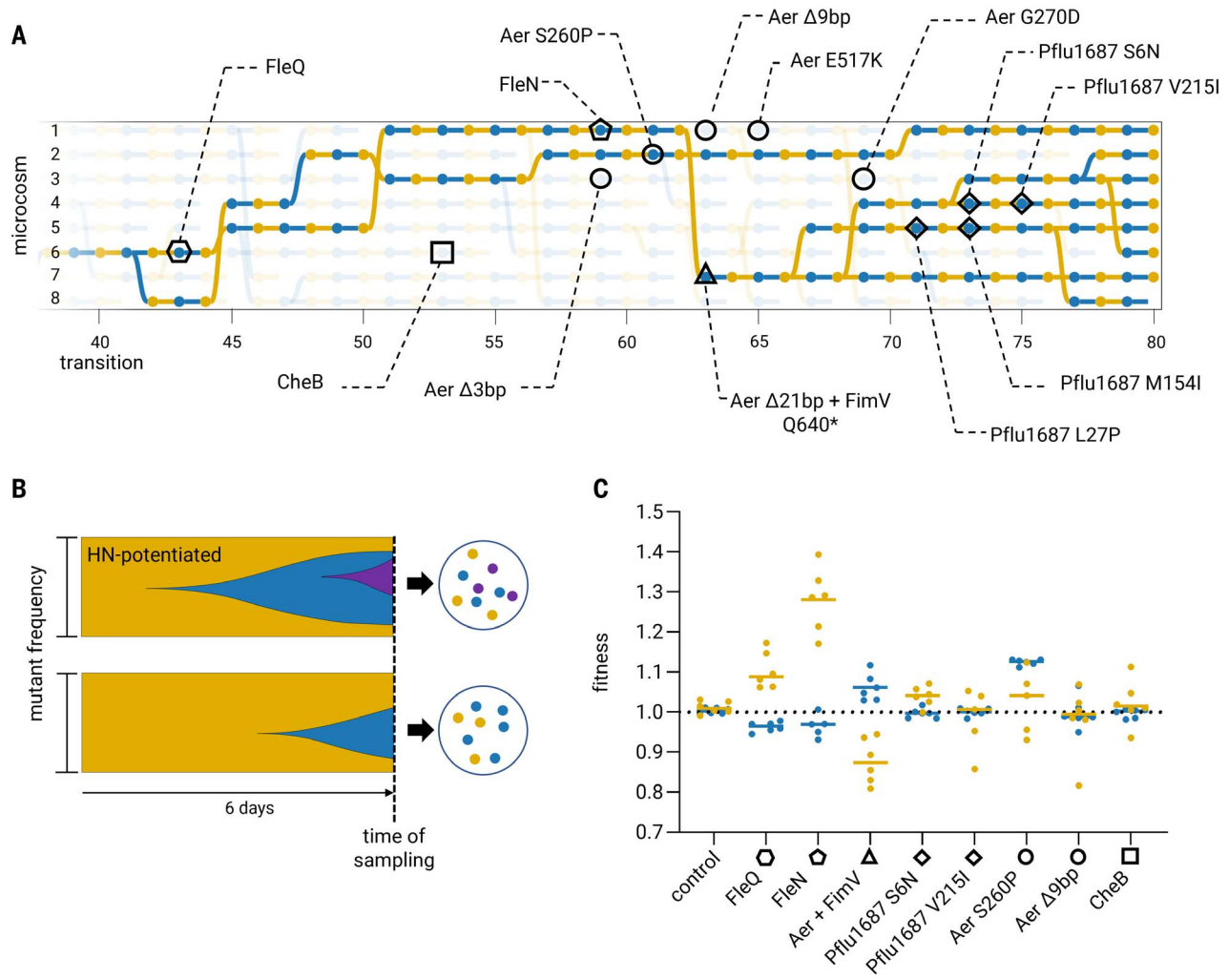

Fig. 6. Secondary mutations and fitness effects. (**A**) Genealogy of successful lineages from metapopulation B between transitions 40 and 80 on which secondary mutations of predicted ecological importance are indicated. (**B**) Muller plots showing predicted consequences of the presence (top) and absence (bottom) of local hypermutation: Early and reliable switching provides an enhanced opportunity for secondary mutations (purple) to reach high frequency (top). (**C**) Fitness consequences of mutations determined by competitive assay against immediate ancestral types in CEL$^+$ (yellow) and CEL$^-$ (blue) backgrounds. Lines indicate mean.

more stringent lineage-level selection pressures. Accordingly, we took a single CEL$^+$ genotype carrying the initial HN duplication (+1 GGTGCCC unit) (T42 M8; open black circle in Fig. 3B) and used this genotype to establish 32 lineages that competed under a restrictive regime where population size was reduced by a factor of 30 and where survival required generation of the target states every 24 hours (Fig. 5).

The selective response, lineage-level dynamics, and changes in numbers of repeats over 10 transitions are revealing. Most lineages managed within 24 hours to achieve the CEL$^-$ state that is required for the first transition, but most did so by losing one copy of the HN sequence. Without exception, those lineages that switched to CEL$^-$ by loss were unable to transition to the CEL$^+$ state during the next 24-hour period and thus went extinct. By contrast, lineages that achieved the CEL$^-$ state (at transition 1) by addition of three HN copies became progenitors of lineages that persisted throughout the course of the experiment. At the end point, lineages harbored, on average, eight additional copies of the HN sequence, with some acquiring as many as 16. A clear association is evident between the number of copies of the HN sequence and the likelihood of survival.

Localized hypermutation facilitates further adaptive evolution

A final observation concerns transitions between phenotypic states in metapopulation B that were associated with multiple mutations. Specifically, we noted that during the 6-day CEL$^+$ to CEL$^-$ period, transitions caused by changes in HN repeat number were more than three times as likely to be associated with additional (secondary) mutations. Of 91 such transitions, 19 harbored secondary mutations (21%). By contrast, of the 167 transitions effected by mutations not involving the HN sequence, only 10 carried secondary mutations (6%) (P = 0.0007, Fisher's exact test, two-tailed).

Although neutral mutations accompanying transition-causing mutations are to be expected (table S2), mutations in loci that encode genes connected to chemotaxis and motility (table S3) may have ecological relevance. Moreover, two loci, the aerotaxis receptor *aer* (*pflu4551*) and a methyl-accepting chemotaxis protein (*pflu1687*), were observed to occur repeatedly (six and four times, respectively) across multiple lineages during transitions mediated by the HN sequence (Fig. 6A). Such parallelism indicated that these mutations were themselves adaptive. Figure 6B elaborates the benefit presumed to accrue to lineages derived from genotypes that switch phenotype early.

To test whether these secondary mutations were adaptive, the fitness effects of a sample of mutations were determined relative to immediate ancestral types, in both the CEL$^+$ and

CEL⁻ backgrounds (Fig. 6C). Following the lineage that descends from T42 M6, the first mutation examined (in T43 M6) was in FleQ [R371C (Arg^{371}→Cys)], a master regulator of motility and polysaccharide production (including cellulose) (*32*, *33*). Relative to the immediate ancestral types, the *fleQ* mutation increased fitness ~10% in CEL⁺ but marginally decreased fitness in CEL⁻. The next mutation, in FleN [L42Q (Leu^{42}→Gln)], which also regulates flagella through interactions with FleQ (*34*), increased fitness of CEL⁺ by a further ~30%, with minimal effects in CEL⁻. Relative to the fitness of T42 M6, the two mutations combined contributed a ~40% fitness gain in CEL⁺.

The genotype at T62 M7 carries two additional mutations (one of only three instances in the experiment where three mutations occurred at the same transition), one a 21–base pair (bp) deletion in Aer and the other a stop codon within FimV [Q640* (Gln^{640}→STOP). These two mutations reduced the fitness of CEL⁺ by ~10% while increasing the fitness of CEL⁻ by ~5%. With the exception of Pflu1687 [S6N (Ser^{6}→Asn) in the CEL⁺ state, no further fitness effects were detected. Secondary mutations in other lineages were also examined, including changes in the chemotaxis protein CheB [T92P (Thr^{92}→Pro)] and further mutations in Aer [S260P (Ser^{260}→Pro) and Δ9bp, a nine-bp deletion], with the largest contribution coming from Aer S260P in the CEL⁻ state. Together, the range of effects shown in Fig. 6C is consistent with the hypothesis that at least some secondary mutations that cooccur with changes in HN repeat number are adaptive.

Discussion

Evolution by natural selection is a blind process, but living systems can appear to possess evolutionary foresight (*20*, *35*). Mechanistically, this is conceivable. Certain configurations of gene regulatory networks (*10*, *11*, *36*), developmental systems (*37*), chromosomal architectures (*15*, *38*), and mutational processes (*16*, *39*) have apparent adaptive utility in future environments. Taking advantage of such future adaptive potential requires not only memory of evolutionary history but often an ability to regenerate previously achieved phenotypic states. In this work, we show how selection on lineages can incorporate prior evolutionary history into the genetic architecture of a single cell, such that mutation appears to anticipate future environmental change.

Central to our findings was a selective process where lineages that were better able to generate adaptive phenotypic variation by mutation replaced those that were less proficient (Fig. 1). In one metapopulation, a single lineage emerged with the capacity to transition rapidly between phenotypic states through expansion and contraction of a short nucleotide repeat in a manner precisely analogous to that of contingency loci in pathogenic bacteria (*16*). Moreover, when multiple lineages of a single genotype carrying the mutational history of 42 previous transitions, but carrying just a single additional copy of the HN sequence, were propagated under a regime that required phenotypic switching on a daily basis, lineages with up to 16 copies of the repeat rapidly evolved (Fig. 5). The derived locus is thus itself highly evolvable with respect to alterations in the frequency of environmental change.

Selection works most forcefully on individuals and is typically weak at higher levels of organization (*6*, *8*, *18*). In our experiments, the death and birth of lineages established a feedback between lineage-level properties and the evolutionary dynamics of cells. Although selection within microcosms favors fast-growing cells, successful lineages were those with the capacity to generate phenotypic variants suited to the future environment. Selection over the doubling time of lineages served to align cell and lineage fitness, precisely as occurs during, for example, the evolutionary transition from cells to multicellular life (*40*).

Throughout our experiment, variation in evolutionary potential between lineages resulted from how adaptive CEL⁺ and CEL⁻ phenotypes were generated by mutation. That a particular history of mutations, with each selected for its immediate benefit to the cell, could culminate in the variation necessary for construction and refinement of a lineage-level adaptation was essential for aligning cell and lineage fitness. This departs from the common assumption, and the basis for doubting the efficacy of selection on evolvability, that evolvability-enhancing mutations deliver no immediate benefit or impose a cost and are therefore susceptible to be lost through drift or purged by selection (*6*, *8*, *41*).

The interplay between mutations conferring immediate benefit to cells and evolvability over the long term (*42*) is illustrated by the mutational history of *pflu0185* that preceded its hypermutator status. A series of mutations leading to elevated *pflu0185* transcription was critical to establishing hypermutability. Each mutation that increased *pflu0185* transcription was selected within microcosms because it generated the adaptive CEL⁻ state. In particular, promoter mutations compensating for previous intragenic loss-of-function mutations that impaired the catalytic activity of Pflu0185 were crucial in ratcheting up transcription. Elevated transcription then potentiated duplication of the HN sequence, consistent with previous observations of transcription-associated mutagenesis (*43*, *44*).

Evidence of additional (secondary) adaptive mutations associated with local hypermutation of *pflu0185* led us to reason that increased propensity to switch enhances the possibility that secondary adaptive mutations, which would otherwise be stalled by the waiting time required to achieve the primary transition-mediating mutation, can increase in frequency (Fig. 6B). Indeed, data presented in Fig. 6 support this hypothesis, showing how the speed of evolution can increase without the threat of Muller's ratchet that arises from global hypermutation (*45*, *46*): The ability to generate adaptive phenotypic variation provides a "head start" to adapt to other aspects of the local environment, with feedback affecting further lineage success.

Finally, we turn to broader implications of the study and particularly the extent to which findings here might have general relevance. The selective regime we used was contrived, with selection on lineages being strictly enforced. Such stringent conditions are likely limited in nature. However, microbial pathogens confronted with the challenge of persistence in the face of the host immune response will experience strong lineage-level selection, with repeated transitions through selective bottlenecks (*47*). As we have shown here, precisely these conditions can promote the evolution of evolvability. That the genomes of obligate pathogenic bacteria are replete with contingency loci bears testimony to this fact. Notably, although each such locus will be constructed through repeated encounters with specific selective environments, possession of multiple loci enables a combinatorial array of phenotypic states that stand to enhance evolvability in novel scenarios [compare (*48*)].

We further suggest that selection on lineages is more important than generally appreciated (*49*). Lineages need only differ in evolutionary potential, for example, in how adaptive phenotypes have been generated by mutation. If they coexist long enough for phenotypic consequences to manifest, then lineages differing in their capacity to generate adaptive variation can compete (*50*–*52*). This is particularly relevant in situations where transmission or migration involves passage through bottlenecks that require variation to be generated afresh (*53*–*55*). Moreover, as we show, if challenges to lineage survival repeat across time, then adaptations that enhance evolvability—shaped by lineage selection for the benefit of lineages—can be expected.

Materials and methods

Experimental evolution

Derivatives of *P. fluorescens* SBW25 were used in all experiments (*26*). Both CEL⁺ and CEL⁻ were propagated in 25-ml glass microcosms containing 6 ml of King's Medium B (KB) at 28°C, without shaking. The four metapopulations were founded by single genotypes derived from a previous, but conceptually similar, experiment (*2*). Founding genotypes carried, on average, nine unique mutations, primarily in characterized cyclic-di-GMP regulators (table S4).

For the CEL$^+$ to CEL$^-$ phase, microcosms were incubated for 6 days and vortexed and then 50 μl of a 3.35×10^5–fold dilution was spread on a KB agar plate. After 48 hours growth, each plate was then examined for the presence of CEL$^-$ colonies, with a single colony used to inoculate a fresh microcosm and initiate a 3-day growth period. One hundred microliters of an 8.0×10^6–fold dilution of each microcosm was plated and screened for CEL$^+$ types. The process was iterated. A random number generator was used to determine the extant lineage that would replace extinct lineages. When an entire metapopulation failed to generate the target state twice over, propagation was ceased (as in metapopulation D). The longer period for the CEL$^+$ to CEL$^-$ transition reflects the time required to first establish the mat that then initiates selection for the CEL$^-$ type. The conditions that favor CEL$^+$, by contrast, arise quickly through rapid depletion of dissolved oxygen and formation of a sharp oxygen gradient at the air-liquid interface.

The births and deaths of lineages were recorded, and the resulting lineage dynamics were visualized using Colgen (*56*). Overnight cultures of each selected CEL$^-$ and CEL$^+$ colony were stored at −80°C in 33% glycerol saline. The "stringent selection" experiment followed the same procedure as above but with cells evolved in 96-well plates containing 200 μl of KB and a reduced period of 24 hours given before dilution and screening.

Sequencing and detection of mutations

Visualization and knowledge of genealogy was used to inform both whole-genome resequencing and targeted Sanger sequencing to detect and order mutational events. For metapopulation B, 482 clones representing successive time points of the experiment were sequenced, allowing precise ordering of mutations underpinning most of the 520 transitions. Remaining transitions and associated mutations were then inferred by parsimony or confirmed by Sanger sequencing. In one instance, to resolve an ambiguity, a mutation (−197 C→T *pflu0185*) was reconstructed to confirm its phenotypic effect.

Genomic DNA was extracted from overnight cultures using the DNeasy DNA Blood and Tissue Kit (Qiagen) according to the manufacturer's spin column protocol. Library preparation and whole-genome sequencing to a depth of ~50× coverage was conducted at either the Max Planck Institute for Evolutionary Biology (Plön, Germany) or Eurofins Genomics (Constance, Germany) using Illumina MiSeq, NextSeq, or NovaSeq. The resulting reads were assembled against the reference *P. fluorescens* SBW25 genome (GenBank accession no. AM181176.4) using the clonal option of Breseq (version 0.35.5) with default parameters (*57*). Mutations were identified with Breseq's HTML output, and, in the case of predicted novel junctions, manually inspected with Geneious Prime. Marginal predictions were confirmed by Sanger sequencing. Polymerase chain reaction (PCR) products for Sanger sequencing were purified with EXOSAP and sequencing conducted by the Max Planck Institute for Evolutionary biology, prepared using the BigDye Terminator v3.1 cycle sequencing kit followed by the BigDye XTerminator purification kit (ThermoFisher) according to the manufacturer's instructions.

Strain construction

Isothermal Gibson Assembly reactions with the NEBuilder HiFi DNA Assembly master mix from New England BioLabs were used for all molecular cloning procedures. Constructs to be integrated into the SBW25 genome contained flanking regions of 400 to 900 bp homologous to the site of integration and were assembled into the transfer plasmid pUISacB (European Nucleotide Archive accession no. OZ219427). Primer overhangs were generated using the online NEBuilder tool (nebuilder.neb.com). All genetic constructs and primers used for construction are available as annotated GenBank files (*27*). All PCRs were performed using master mixes of high-fidelity polymerases (Phusion or Q5) and purified with the QIAquick PCR purification kit (Qiagen). pUISacB was extracted from overnight cultures using the QIAprep Spin Miniprep Kit (Qiagen), linearized with Spe I, amplified by PCR and digested with Dpn I to remove remaining plasmid template. Assembled constructs were transformed into chemically competent *Escherichia coli* Top 10 cells and integrated into SBW25 by two-step allelic exchange, as previously described (*58*), but with final mutant selection using sucrose counterselection on tryptone yeast extract and sucrose (TYS10) plates (10 g/liter tryptone, 5 g/liter yeast extract, 10% (w/v) filtered sucrose, 15 g/liter agar).

For the *pflu0185* "frameshift detector" used to measure local frameshift rate, a fusion was constructed with *kanR* via the linker sequence "GCTAGCAGCGCAAGCGCAAGCGCA" (ASSASASA), such that the latter gene was 1 bp out of frame with respect to *pflu0185* (an in-frame version of the same *kanR* fusion was also constructed). Three synonymous mutations engineered into the 5′ end of *kanR* were required to remove aberrant start codons that existed in the out-of-frame sequence (which otherwise restarted the correct reading frame). For confirmation that the increase in frameshift rate correlating with transcription of *pflu0185* reflected a local effect, we assembled an out-of-frame *kanR* fusion with the wild-type *pflu0185* sequence into pUC18R6K-mini-Tn*7*T-Gm (*59*) and transformed this along with the helper plasmid pUX-BF13 (containing transposition machinery) (*60*) into derived SBW25 through electroporation, as previously described (*59*).

Transposon mutagenesis

Transposon mutagenesis using Tn*5* was conducted according to the previously described method (*58*). Briefly, this involved a triparental conjugation between the recipient CEL$^+$ and an *E. coli* donor containing the plasmid pCM639 with the IS-Ω-kan/hah transposon along with *E. coli* containing the helper plasmid pRK2013. Suppressor mutants were identified by screening for CEL$^-$ colonies. The site of insertion was determined by amplifying the transposon-chromosome junction through arbitrarily primed PCR with Sanger sequencing of the resulting product.

Minimum inhibitory concentrations

MIC, used as a proxy for transcription, was determined by plating ~10^8 cells of the relevant genotypes engineered with an in-frame *pflu0185-kanR* fusion onto KB agar and applying a kanamycin MIC test strip (Liofilchem). After 24 hours of growth, the MIC was determined by identifying where the margin of growth intercepted the strip in three independent replicates. In cases where genotypes exhibited high levels of resistance extending beyond the maximum measurable range of the test strips (256 μg/ml, the assay was instead conducted on KB agar containing either 100 or 200 μg/ml of kanamycin and the concentrations were summed.

Fluctuation assays

Colony counts on selective and nonselective plates were used to estimate mutation rates using the rSalvador R package (v1.9), which generates a maximum likelihood estimate of mutation rate under the Luria-Delbruck model while accounting for variation in plating efficiency (*61*). The likelihood ratio method was used to calculate confidence intervals and the statistical significance of differences between mutation rate estimates. Global mutation rates were assessed using rifampicin (100 μg/ml) and kanamycin (at concentrations of 5 to 50 μg/ml depending on *pflu0185* expression) used to determine rates of frameshifting within *pflu0185*. Twelve independent cultures were used to determine spontaneous mutants; six were used to determine population size. To minimize confounding fitness differences between CEL$^-$ and CEL$^+$ states, all strains used for *pflu0185* frameshifting fluctuation assays were modified with a cellulose-inactivating mutation (WssEΔ993L-1260E) so that cells maintained the CEL$^-$ state.

Fitness assays

Fitness was measured by 1:1 competition across six biological replicates in either static (for CEL$^+$) or shaken (for CEL$^-$) microcosms. Shaking microcosms were used as a proxy environment for CEL$^-$ because of the difficulty of reconstituting the selective conditions of growth within a CEL$^+$

mat. Competitors were fluorescently marked with either mScarlet-I or sGFP2 and were otherwise isogenic but for the secondary mutation of interest. The control consisted of a single representative CEL$^-$ or CEL$^+$ strain with both fluorescent markers competed against itself. Starting populations were derived from colonies inoculated into KB microcosms and grown 24 hours at 28°C in a shaking incubator. Microcosms were then vortexed and, in the case of CEL$^+$ strains, sonicated (Bandelin Sonopuls mini 20: 2-mm probe, 80% amplitude, 20-s duration) to further break up cell aggregates. Competitors were then mixed 1:1 and diluted in filtered phosphate buffered saline (PBS) (0.22-μM filter), with the initial ratio of fluorescent events obtained using flow cytometry (MACSQuant VYB). Six microliters of the 1:1 mix was also used to initiate competitions, which ran for either 24 (shaken) or 48 (static) hours. After competitive growth, microcosms were vortexed (and static CEL$^+$ microcosms again sonicated) and diluted in filtered PBS, and the final ratios were determined by flow cytometry. Fitness was calculated as the ratio of Malthusian parameters (*62*).

REFERENCES AND NOTES

1. P. D. Sniegowski, P. J. Gerrish, R. E. Lenski, Evolution of high mutation rates in experimental populations of *E. coli*. *Nature* **387**, 703–705 (1997). doi: 10.1038/42701; pmid: 9192894
2. K. Hammerschmidt, C. J. Rose, B. Kerr, P. B. Rainey, Life cycles, fitness decoupling and the evolution of multicellularity. *Nature* **515**, 75–79 (2014). doi: 10.1038/nature13884; pmid: 25373677
3. M. Amicone *et al*., Mutation rate of SARS-CoV-2 and emergence of mutators during experimental evolution. *Evol. Med. Public Health* **10**, 142–155 (2022). doi: 10.1093/emph/eoac010; pmid: 35419205
4. M. Lescat *et al*., Using long-term experimental evolution to uncover the patterns and determinants of molecular evolution of an *Escherichia coli* natural isolate in the streptomycin-treated mouse gut. *Mol. Ecol.* **26**, 1802–1817 (2017). doi: 10.1111/mec.13851; pmid: 27661780
5. F. Taddei *et al*., Role of mutator alleles in adaptive evolution. *Nature* **387**, 700–702 (1997). doi: 10.1038/42696; pmid: 9192893
6. P. D. Sniegowski, H. A. Murphy, Evolvability. *Curr. Biol.* **16**, R831–R834 (2006). doi: 10.1016/j.cub.2006.08.080; pmid: 17027474
7. M. Pigliucci, Is evolvability evolvable? *Nat. Rev. Genet.* **9**, 75–82 (2008). doi: 10.1038/nrg2278; pmid: 18059367
8. M. Lynch, The frailty of adaptive hypotheses for the origins of organismal complexity. *Proc. Natl. Acad. Sci. U.S.A.* **104**, 8597–8604 (2007). doi: 10.1073/pnas.0702207104; pmid: 17494740
9. A. Stoltzfus, *Mutation, Randomness, and Evolution* (Oxford Univ. Press, 2021). doi: 10.1093/oso/9780198844457.001.0001
10. R. A. Watson, G. P. Wagner, M. Pavlicev, D. M. Weinreich, R. Mills, The evolution of phenotypic correlations and "developmental memory". *Evolution* **68**, 1124–1138 (2014). doi: 10.1111/evo.12337; pmid: 24351058
11. A. Crombach, P. Hogeweg, Evolution of evolvability in gene regulatory networks. *PLOS Comput. Biol.* **4**, e1000112 (2008). doi: 10.1371/journal.pcbi.1000112; pmid: 18617989
12. N. Kashtan, E. Noor, U. Alon, Varying environments can speed up evolution. *Proc. Natl. Acad. Sci. U.S.A.* **104**, 13711–13716 (2007). doi: 10.1073/pnas.0611630104; pmid: 17698964
13. R. Canino-Koning, M. J. Wiser, C. Ofria, Fluctuating environments select for short-term phenotypic variation leading to long-term exploration. *PLOS Comput. Biol.* **15**, e1006445 (2019). doi: 10.1371/journal.pcbi.1006445; pmid: 31002665
14. J. Draghi, G. P. Wagner, Evolution of evolvability in a developmental model. *Evolution* **62**, 301–315 (2008). doi: 10.1111/j.1558-5646.2007.00303.x; pmid: 18031304
15. E. S. Colizzi, B. van Dijk, R. M. H. Merks, D. E. Rozen, R. M. A. Vroomans, Evolution of genome fragility enables microbial division of labor. *Mol. Syst. Biol.* **19**, e11353 (2023). doi: 10.15252/msb.202211353; pmid: 36727665
16. E. R. Moxon, P. B. Rainey, M. A. Nowak, R. E. Lenski, Adaptive evolution of highly mutable loci in pathogenic bacteria. *Curr. Biol.* **4**, 24–33 (1994). doi: 10.1016/S0960-9822(00)00005-1; pmid: 7922307
17. C. D. Bayliss, D. Field, E. R. Moxon, The simple sequence contingency loci of *Haemophilus influenzae* and *Neisseria meningitidis*. *J. Clin. Invest.* **107**, 657–662 (2001). doi: 10.1172/JCI12557; pmid: 11254662
18. G. C. Williams, *Adaptation and Natural Selection: A Critique of Some Current Evolutionary Thought*, **vol. 61** (Princeton Univ. Press, 1966).
19. R. C. Lewontin, The units of selection. *Annu. Rev. Ecol. Syst.* **1**, 1–18 (1970). doi: 10.1146/annurev.es.01.110170.000245
20. R. Dawkins, "The evolution of evolvability" in *Artificial Life: Proceedings of an Interdisciplinary Workshop on the Synthesis and Simulation of Living Systems*, C. Langton, Ed. (Routledge, 1989), pp. 201–220.
21. N. Virgo, E. Agmon, C. Fernando, "Lineage selection leads to evolvability at large population sizes" in *Proceedings of the Fourteenth European Conference on Artificial Life* (ASME, 2017), pp. 420–427.
22. I. Eshel, Clone selection and the evolution of modifying features. *Theor. Popul. Biol.* **4**, 196–208 (1973). doi: 10.1016/0040-5809(73)90029-4
23. G. Bell, *Selection: The Mechanism of Evolution* (Oxford Univ. Press, 2008).
24. M. Conrad, Bootstrapping on the adaptive landscape. *Biosystems* **11**, 167–182 (1979). doi: 10.1016/0303-2647(79)90009-1; pmid: 497367
25. L. Nunney, "Lineage selection: Natural selection for long-term benefit" in *Levels of Selection in Evolution*, L. Keller, Ed. (Princeton University Press, 1999), pp. 238–252.
26. P. B. Rainey, M. Travisano, Adaptive radiation in a heterogeneous environment. *Nature* **394**, 69–72 (1998). doi: 10.1038/27900; pmid: 9665128
27. M. Barnett, Evolvability, Version 1. Edmond (2024); doi: 10.17617/3.5PEE52
28. G. Levinson, G. A. Gutman, Slipped-strand mispairing: A major mechanism for DNA sequence evolution. *Mol. Biol. Evol.* **4**, 203–221 (1987). pmid: 3328815
29. R. Simm, M. Morr, A. Kader, M. Nimtz, U. Römling, GGDEF and EAL domains inversely regulate cyclic di-GMP levels and transition from sessility to motility. *Mol. Microbiol.* **53**, 1123–1134 (2004). doi: 10.1111/j.1365-2958.2004.04206.x; pmid: 15306016
30. Y.-M. Cai *et al*., The c-di-GMP phosphodiesterase PipA (PA0285) regulates autoaggregation and Pf4 bacteriophage production in *Pseudomonas aeruginosa* PAO1. *Appl. Environ. Microbiol.* **88**, e00039-22 (2022). doi: 10.1128/aem.00039-22; pmid: 35638845
31. A. Datta, S. Jinks-Robertson, Association of increased spontaneous mutation rates with high levels of transcription in yeast. *Science* **268**, 1616–1619 (1995). doi: 10.1126/science.7777859; pmid: 7777859
32. J. W. Hickman, C. S. Harwood, Identification of FleQ from *Pseudomonas aeruginosa* as a c-di-GMP-responsive transcription factor. *Mol. Microbiol.* **69**, 376–389 (2008). doi: 10.1111/j.1365-2958.2008.06281.x; pmid: 18485075
33. S. R. Giddens *et al*., Mutational activation of niche-specific genes provides insight into regulatory networks and bacterial function in a complex environment. *Proc. Natl. Acad. Sci. U.S.A.* **104**, 18247–18252 (2007). doi: 10.1073/pnas.0706739104; pmid: 17989226
34. N. Dasgupta, R. Ramphal, Interaction of the antiactivator FleN with the transcriptional activator FleQ regulates flagellar number in *Pseudomonas aeruginosa*. *J. Bacteriol.* **183**, 6636–6644 (2001). doi: 10.1128/JB.183.22.6636-6644.2001; pmid: 11673434
35. P. Hogeweg, Toward a theory of multilevel evolution: Long-term information integration shapes the mutational landscape and enhances evolvability. *Adv. Exp. Med. Biol.* **751**, 195–224 (2012). pmid: 22821460
36. G. P. Wagner, L. Altenberg, Perspective: Complex adaptations and the evolution of evolvability. *Evolution* **50**, 967–976 (1996). doi: 10.2307/2410639; pmid: 28565291
37. M. Kirschner, J. Gerhart, Evolvability. *Proc. Natl. Acad. Sci. U.S.A.* **95**, 8420–8427 (1998). doi: 10.1073/pnas.95.15.8420; pmid: 9671692
38. J. W. Pepper, The evolution of evolvability in genetic linkage patterns. *Biosystems* **69**, 115–126 (2003). doi: 10.1016/S0303-2647(02)00134-X; pmid: 12689725
39. C. J. Graves, V. I. Ros, B. Stevenson, P. D. Sniegowski, D. Brisson, Natural selection promotes antigenic evolvability. *PLOS Pathog.* **9**, e1003766 (2013). doi: 10.1371/journal.ppat.1003766; pmid: 24244173
40. A. J. Black, P. Bourrat, P. B. Rainey, Ecological scaffolding and the evolution of individuality. *Nat. Ecol. Evol.* **4**, 426–436 (2020). doi: 10.1038/s41559-019-1086-9; pmid: 32042121
41. W. J. Dickinson, J. Seger, Cause and effect in evolution. *Nature* **399**, 30 (1999). doi: 10.1038/19894; pmid: 10331386
42. A. Wagner, Adaptive evolvability through direct selection instead of indirect, second-order selection. *J. Exp. Zool. B Mol. Dev. Evol.* **338**, 395–404 (2022). doi: 10.1002/jez.b.23071; pmid: 34254439
43. M. Wierdl, C. N. Greene, A. Datta, S. Jinks-Robertson, T. D. Petes, Destabilization of simple repetitive DNA sequences by transcription in yeast. *Genetics* **143**, 713–721 (1996). doi: 10.1093/genetics/143.2.713; pmid: 8725221
44. M. Zavodna, A. Bagshaw, R. Brauning, N. J. Gemmell, The effects of transcription and recombination on mutational dynamics of short tandem repeats. *Nucleic Acids Res.* **46**, 1321–1330 (2018). doi: 10.1093/nar/gkx1253; pmid: 29300948
45. P. D. Sniegowski, P. J. Gerrish, T. Johnson, A. Shaver, The evolution of mutation rates: Separating causes from consequences. *BioEssays* **22**, 1057–1066 (2000). doi: 10.1002/1521-1878(200012)22:12<1057::AID-BIES3>3.0.CO;2-W; pmid: 11084621
46. A. Couce, J. R. Guelfo, J. Blázquez, Mutational spectrum drives the rise of mutator bacteria. *PLOS Genet.* **9**, e1003167 (2013). doi: 10.1371/journal.pgen.1003167; pmid: 23326242
47. R. Moxon, E. Kussell, The impact of bottlenecks on microbial survival, adaptation, and phenotypic switching in host-pathogen interactions. *Evolution* **71**, 2803–2816 (2017). doi: 10.1111/evo.13370; pmid: 28983912
48. M. Parter, N. Kashtan, U. Alon, Facilitated variation: How evolution learns from past environments to generalize to new environments. *PLOS Comput. Biol.* **4**, e1000206 (2008). doi: 10.1371/journal.pcbi.1000206; pmid: 18989390
49. C. J. Graves, D. M. Weinreich, Variability in fitness effects can preclude selection of the fittest. *Annu. Rev. Ecol. Evol. Syst.* **48**, 399–417 (2017). doi: 10.1146/annurev-ecolsys-110316-022722; pmid: 31572069
50. D. Woods *et al*., Diverse and robust molecular algorithms using reprogrammable DNA self-assembly. *Nature* **567**, 366–372 (2019). doi: 10.1038/s41586-019-1014-9; pmid: 30894725
51. J. T. Ferrare, B. H. Good, Evolution of evolvability in rapidly adapting populations. *Nat. Ecol. Evol.* **8**, 2085–2096 (2024). doi: 10.1038/s41559-024-02527-0; pmid: 39261599
52. D. Leon, S. D'Alton, E. M. Quandt, J. E. Barrick, Innovation in an *E. coli* evolution experiment is contingent on maintaining adaptive potential until competition subsides. *PLOS Genet.* **14**, e1007348 (2018). doi: 10.1371/journal.pgen.1007348; pmid: 29649242
53. A. K. Lancaster, J. Masel, The evolution of reversible switches in the presence of irreversible mimics. *Evolution* **63**, 2350–2362 (2009). doi: 10.1111/j.1558-5646.2009.00729.x; pmid: 19486147
54. E. Libby, P. B. Rainey, Exclusion rules, bottlenecks and the evolution of stochastic phenotype switching. *Proc. Biol. Sci.* **278**, 3574–3583 (2011). doi: 10.1098/rspb.2011.0146; pmid: 21490013
55. H. J. Beaumont, J. Gallie, C. Kost, G. C. Ferguson, P. B. Rainey, Experimental evolution of bet hedging. *Nature* **462**, 90–93 (2009). doi: 10.1038/nature08504; pmid: 19890329
56. G. Doulcier, P. Remigi, D. Rexin, P. B. Rainey, Evolutionary dynamics of nascent multicellular lineages. bioRxiv 2024.05.10.593459 [Preprint] (2024); https://doi.org/10.1101/2024.05.10.593459.
57. J. E. Barrick *et al*., Identifying structural variation in haploid microbial genomes from short-read resequencing data using breseq. *BMC Genomics* **15**, 1039 (2014). doi: 10.1186/1471-2164-15-1039; pmid: 25432719
58. E. Bantinaki *et al*., Adaptive divergence in experimental populations of *Pseudomonas fluorescens*. III. Mutational origins of wrinkly spreader diversity. *Genetics* **176**, 441–453 (2007). doi: 10.1534/genetics.106.069906; pmid: 17339222

59. K.-H. Choi, H. P. Schweizer, mini-Tn7 insertion in bacteria with single attTn7 sites: Example *Pseudomonas aeruginosa*. *Nat. Protoc.* **1**, 153–161 (2006). doi: 10.1038/nprot.2006.24; pmid: 17406227
60. Y. Bao, D. P. Lies, H. Fu, G. P. Roberts, An improved Tn7-based system for the single-copy insertion of cloned genes into chromosomes of gram-negative bacteria. *Gene* **109**, 167–168 (1991). doi: 10.1016/0378-1119(91)90604-A; pmid: 1661697
61. Q. Zheng, rSalvador: an R package for the fluctuation experiment. *G3* **7**, 3849–3856 (2017). doi: 10.1534/g3.117.300120; pmid: 29084818
62. R. E. Lenski, M. R. Rose, S. C. Simpson, S. C. Tadler, Long-term experimental evolution in *Escherichia coli*. I. Adaptation and divergence during 2,000 generations. *Am. Nat.* **138**, 1315–1341 (1991). doi: 10.1086/285289
63. P. Domínguez-Cuevas, S. Marqués, "Compiling sigma-70-dependent promoters" in *Virulence Gene Regulation*, J.-L. Ramos Ed. (Springer, 2004), pp. 319–343.
64. C. A. Vakulskas, K. M. Brady, T. L. Yahr, Mechanism of transcriptional activation by *Pseudomonas aeruginosa* ExsA. *J. Bacteriol.* **191**, 6654–6664 (2009). doi: 10.1128/JB.00902-09; pmid: 19717612

ACKNOWLEDGMENTS

We acknowledge generous core support from the Max Planck Society and thank members of the Department of Microbial Population Biology for help, ideas, and discussion and Alina Waldmann for genomic DNA purification. We are grateful to D. Rogers for insight into the mechanism by which the HN repeat achieves the first duplication and for the suggestion of a strategy for measuring frameshift mutations. We are also indebted to R. Moxon for valuable comments and discussion. **Funding:** This work was funded by Max Planck Society core funding. **Author contributions:** Experimental concept and design: M.B., P.B.R.; Experimental work and analysis: M.B.; Technical assistance: L.M.; Writing of manuscript: M.B., P.B.R. **Competing interests:** The authors declare that they have no competing interests. **Data and materials availability:** All data are available in the manuscript or supplementary materials or are retrievable from Edmond (*27*). All genetic data and the full history of metapopulation B in the form of an interactive tree can be explored online (*27*).

SUPPLEMENTARY MATERIALS

science.org/doi/10.1126/science.adr2756
Figs. S1 to S6
Tables S1 to S4
References
MDAR Reproducibility Checklist
Movie S1

Submitted 24 June 2024; resubmitted 30 July 2024
Accepted 11 December 2024
10.1126/science.adr2756